

Network-of-queues approach to B-cell-receptor affinity discrimination

Federico Felizzi* and Federico Comoglio†

*Department of Biosystems Science and Engineering, Swiss Federal Institute of Technology (ETH) Zurich,
Mattenstrasse 26, CH-4058 Basel, Switzerland*

(Received 15 December 2011; revised manuscript received 21 April 2012; published 28 June 2012)

The immune system is one of the most complex signal processing machineries in biology. The adaptive immune system, consisting of B and T lymphocytes, is activated in response to a large spectrum of pathogen antigens. B cells recognize and bind the antigen through B-cell receptors (BCRs) and this is fundamental for B-cell activation. However, the system response is dependent on BCR-antigen affinity values that span several orders of magnitude. Moreover, the ability of the BCR to discriminate between affinities at the high end (e.g., $10^9 M^{-1}$ – $10^{10} M^{-1}$) challenges the formulation of a mathematical model able to robustly separate these affinity-dependent responses. Queuing theory enables the analysis of many related processes, such as those resulting from the stochasticity of protein binding and unbinding events. Here we define a network of queues, consisting of BCR early signaling states and transition rates related to the propensity of molecular aggregates to form or disassemble. By considering the family of marginal distributions of BCRs in a given signaling state, we report a significant separation (measured as Jensen-Shannon divergence) that arises from a broad spectrum of antigen affinities.

DOI: [10.1103/PhysRevE.85.061926](https://doi.org/10.1103/PhysRevE.85.061926)

PACS number(s): 87.16.Xa

I. INTRODUCTION

The immune system is a complex biological machinery consisting of innate and adaptive systems that has evolved to defend our organism from foreign invaders. The innate immune system provides a first line of defense which nonspecifically recognizes pathogen-associated molecules globally called antigens and activates the adaptive immune response. This first step ensures that a destructive response is triggered only against foreign antigens (non-self) and not against molecules of the host itself (self). The adaptive immune system consists of white blood cells called lymphocytes. Different types of lymphocytes, known as B cells and T cells, play different roles in the immune response. B cells, the focus of this work, are responsible for antibody-mediated responses, whereas T cells carry out cell-mediated responses [1].

A key feature of the adaptive immune system is its ability to respond to a large number of different antigens with high specificity. The clonal selection theory [2] shed light on how this can be achieved by proposing that specificity for diverse antigens already exists before they are encountered [3]. Initially, the organism generates a pool of lymphocytes that can recognize antigens through cell-type-specific receptors, e.g., B-cell receptors (BCRs) for B cells [4]. BCR binding to antigen leads to B-cell proliferation and clonal expansion, thus producing effector cells that are clones of the activated lymphocyte bearing the same antigen-specific BCR. Activated B cells secrete antibodies in the bloodstream to specifically recognize the foreign antigen that initiates their production. However, how a specific antibody is selected, given the magnitude of molecularly diverse antigens, is still unclear. Additionally, the affinity range over which B cells can recognize antigens spans several orders of magnitude [5] and different affinity values induce different

cellular responses [6]. Upon antigen binding [Fig. 1(a)–1(b)], target sequences in the immunoreceptor tyrosine-based activation motifs (ITAMs) of the BCR signaling subunits $Ig\alpha$ and $Ig\beta$ are phosphorylated by the Src-family protein tyrosine kinase Lyn and the cytoplasmic tyrosine kinase Syk (spleen tyrosine kinase) [7] [Fig. 1(b)]. These processes are stochastic and therefore they represent an intrinsic source of noise [8].

Various approaches modeled the dependence of B-cell activation on antigen concentration and affinity. In Ref. [9], an affinity-dependent increase of the B-cell surface enhances the formation of BCR microclusters. While such spreading response can amplify affinity sensitivity, little is known on how B cells exploit membrane-proximal signaling to discriminate among affinities at the level of microclusters. Recent studies [6,10] provide novel, yet contrasting, interpretations on this phenomenon. To our knowledge, the mechanism of BCR affinity discrimination has been addressed using a time threshold for a kinetic proofreading scheme involving BCR-antigen binding and activated Lyn and Syk kinases [11]. Kinetic proofreading models have been applied in immunology after the seminal work of McKeithan [12]. The model accounts for activation and deactivation rates of a series of biochemical reactions occurring at receptor tails under the assumption that upon antigen unbinding the receptor jumps back to the native state regardless of its biochemical modifications. In [11] well-defined transition rates tuned for the discrete stochastic model have been proposed, with binding or unbinding events implicitly modeled as geometric random variables. This model has two major limitations. First, kinetic proofreading was simulated *ad hoc* by introducing a deterministic time threshold t for BCR-antigen binding that has to be exceeded before the BCR could engage cytoplasmic signaling molecules. However, when t is neglected the model is not able to separate affinity-dependent responses for high affinity values. Second, despite a careful parametrization a large number of simulations is required in order to obtain statistically relevant results.

In this work we propose a model that captures the orchestrated behavior of many molecules of different types,

*federico.felizzi@bsse.ethz.ch

†Also at Life Science Zurich Graduate School, Ph.D. program in Systems Biology.

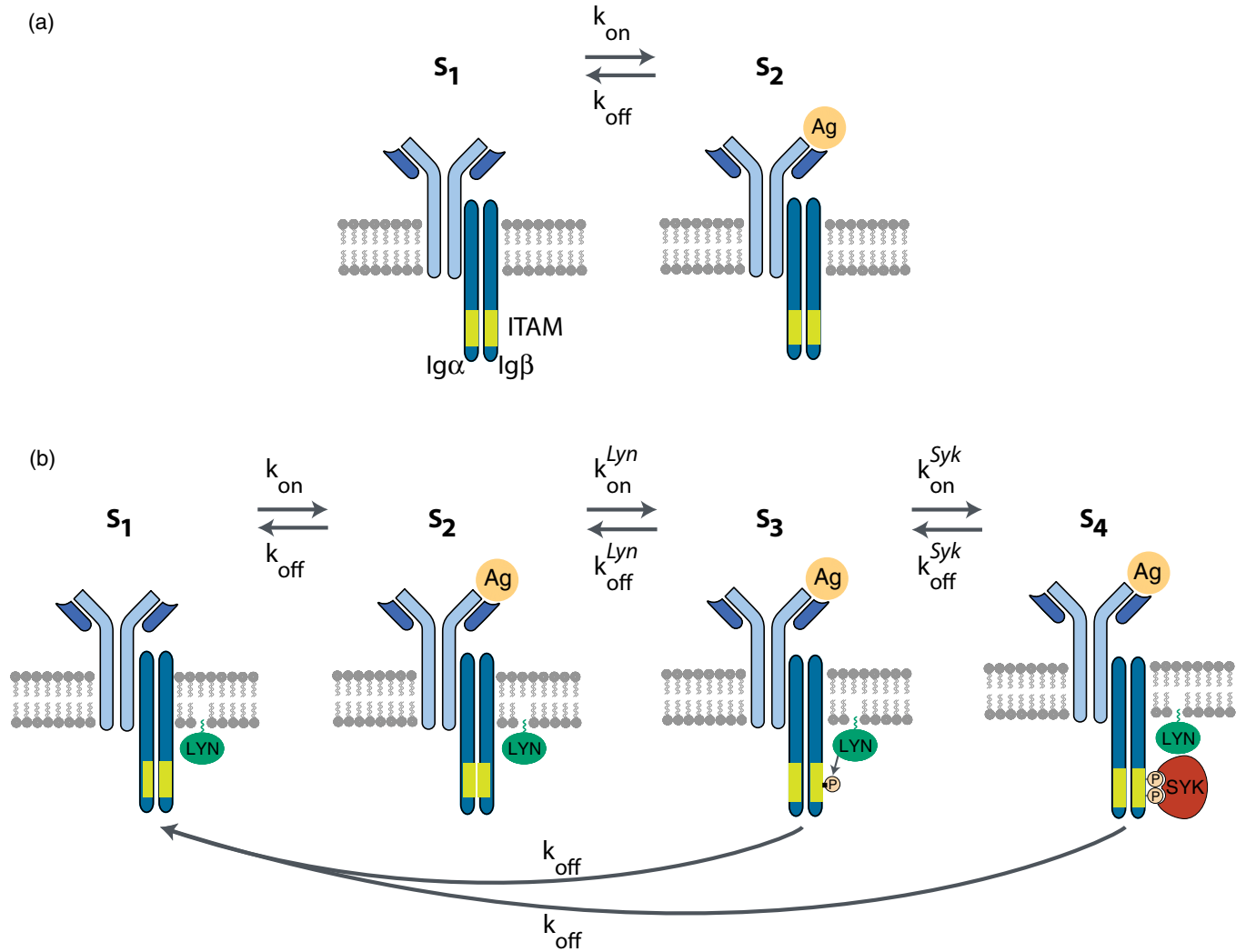


FIG. 1. (Color online) (a) Simplified signaling pathway, consisting of two states (s_1 and s_2). s_1 provides a schematic representation of a BCR. Heavy and light BCR chains are colored in light blue and blue, respectively. BCR signaling subunits $Ig\alpha$ and $Ig\beta$ are represented in dark blue. The ITAMs are indicated. Transitions between states are indicated by arrows and modulated by the reported parameters. (b) Upon BCR binding to antigen (Ag), target sequences in the ITAMs are phosphorylated by Lyn (s_3) and Syk (s_4). We assume that antigen unbinding is nonreversible, i.e., the receptor reverts to s_1 , regardless of the state it was or is in.

leading to a more robust detection of different binding affinities when compared with modifications applied at the receptor level only. Our method avoids deterministic time thresholds nevertheless delivering results in agreement with both *in silico* observations and experimental results reported in Ref. [11]. The method exploits ideas outlined for T-cell receptors (TCRs) [13], where each compartment of the kinetic proofreading scheme is described as a queue. By combining time thresholds and signal integration, the model in Ref. [13] is able to explain T-cell specificity for different antigen densities. However, k_{off} does not span several orders of magnitude. A similar queuing scheme was applied to the TCR recognition of self and non-self antigens, where T cells were modeled as decision makers in this discrimination process [14].

In our framework, the spatial component is not modeled explicitly, although spatial proximity of reacting species influences the rates of binding events. We rather assume that there are several foci where BCRs assemble [9,15] and we focus on the transition steps taking place within the assembly zone.

This paper is organized as follows. Sec. II introduces the modeling framework and the relevant formalism. In Sec. II A we consider the marginal distributions of receptors in a given state. The distance between probability distributions arising from different BCR-antigen affinity values is analyzed in Sec. II B. In Sec. III A, we choose the model parameter based on experimental results, and sensitivity of the model with respect to alterations of other parameter values is discussed in Sec. III B. In Sec. III C, a simplified signaling pathway is examined. Finally, Sec. III D analyzes the affinity discrimination ability as a function of the number of BCRs in the system.

II. MODEL

In the following, we introduce the formalism required to understand the network of queues and analyze their behavior. Due to their similarity to kinetic proofreading models [12], network queuing systems can prove useful in solving biological

problems. We model the behavior of BCRs in the system as a closed migration process [16]. Briefly, a closed migration process consists of a set $\mathcal{S} = \{1, 2, \dots, S\}$ of colonies, a vector $\mathbf{n} = (n_1, n_2, \dots, n_S)$ defining the number of elements belonging to each of the S colonies, and an operator T_{ij} on \mathbf{n} defined as follows:

$$T_{ij}(\mathbf{n}) = (\dots, n_i - 1, \dots, n_j + 1, \dots). \quad (1)$$

In words, the operator $T_{ij}(\mathbf{n})$ removes one element from colony i and adds it to colony j . The term closed indicates that elements cannot enter or leave the system, i.e., the total number of elements is fixed to be N . Notice that the term migration does not refer to physical movement. In our application to BCRs, elements are receptors and colonies are the states in which a receptor can be. The vector \mathbf{n} is assumed to be a Markov process with state space:

$$\mathcal{N} = \{\mathbf{n} : n_s \geq 0, s = 1, \dots, S, \mathbf{1}^T \mathbf{n} = N\} \quad (2)$$

and transition rates given by

$$q(\mathbf{n}, T_{ij}(\mathbf{n})) = \lambda_{ij} \phi_i(n_i), \quad (3)$$

where λ_{ij} is the propensity for an element in the system to transit from colony i to colony j and $\phi_i(n_i)$ are monotonic increasing functions of n_i . Such a Markov process \mathbf{n} is irreducible if $\phi_i(n) > 0$ whenever $n > 0$ and the topology of the network describing the transitions from one colony to another is such that for any pair of colonies (i, j) transitions between the two colonies happen almost surely. We assume that the times at which binding and unbinding events occur follow an exponential distribution [17]. Under these assumptions, we model the behavior of BCRs in the system as ‘‘customers’’ joining a queue. Each receptor then waits in the queue until the next event takes place. Such event typically consists in the binding or unbinding of either the antigen or a signaling protein and this causes the receptor to join another queue, i.e., to transit to another colony. Experimental investigations of the BCR system and of early events in B-cell activation [6,18,19]

suggested us to construct a network of queues consisting of four states: (1) s_1 : unbound BCR, (2) s_2 : BCR bound to antigen, (3) s_3 : BCR bound to Lyn, and (4) s_4 : BCR bound to both Lyn and Syk.

We fix the number of receptors N within a given surface area and for simplicity we do not add any further constraints on other quantities. The total number of antigen, Lyn, and Syk molecules is assumed to exceed the total number of signaling engaged BCRs (Table II) to prevent an insufficient allocation of resources in the system [20].

Transitions from one state to another can be defined as follows:

$$q(\mathbf{n}, T_{ij}(\mathbf{n})) = \begin{cases} k_{\text{on}} \phi_i(n_i), & i = 1, j = 2 \\ k_{\text{on}}^{\text{Lyn}} \phi_i(n_i), & i = 2, j = 3 \\ k_{\text{on}}^{\text{Syk}} \phi_i(n_i), & i = 3, j = 4 \\ k_{\text{off}}^{\text{Lyn}} \phi_i(n_i), & i = 3, j = 2 \\ k_{\text{off}}^{\text{Syk}} \phi_i(n_i), & i = 4, j = 3 \\ k_{\text{off}} \phi_i(n_i), & i \in \{2, 3, 4\}, j = 1 \end{cases}.$$

According to experimental results [18], we set $\phi_{1,2,3}(n) = n$ and $\phi_4(n) = n^q$, where $q > 1$. The choice for colonies 1, 2, 3 follows from the fact that transitions between them are independent of the elements within these colonies. However, recruitment of the Syk kinase to the modified BCR tail (s_4) is connected to downstream signaling pathways and contributes to cytoskeleton organization [18]. Thus, we hypothesize that transitions leaving s_4 depend on the number of BCRs in s_4 .

Next, we turn our attention to the analysis of steady state distributions of elements at each colony as a function of the BCR-antigen affinity, namely, on the unbinding rate k_{off} . This is in line with considerations that differences in the antigen affinity $K_D = \frac{k_{\text{on}}}{k_{\text{off}}}$ are considered to be functional differences related to k_{off} and not to k_{on} [21,22]. For this purpose, we construct the generator of the continuous time Markov chain describing the behavior of a single receptor in the system as

$$H = \begin{bmatrix} -k_{\text{on}} & k_{\text{on}} & 0 & 0 \\ k_{\text{off}} & -k_{\text{off}} - k_{\text{on}}^{\text{Lyn}} & k_{\text{on}}^{\text{Lyn}} & 0 \\ k_{\text{off}} & k_{\text{off}}^{\text{Lyn}} & -k_{\text{off}} - k_{\text{off}}^{\text{Lyn}} - k_{\text{on}}^{\text{Syk}} & k_{\text{on}}^{\text{Syk}} \\ k_{\text{off}} & 0 & k_{\text{off}}^{\text{Syk}} & -k_{\text{off}} - k_{\text{off}}^{\text{Syk}} \end{bmatrix}, \quad (4)$$

and we compute the equilibrium distribution $\alpha = (\alpha_i)$ as

$$H^T \alpha = 0, \quad (5)$$

which is equivalent to say that α satisfies the full balance equations [16,23]. Under the above mentioned assumptions the equilibrium distribution π of the process \mathbf{n} satisfies [16]

$$\pi(\mathbf{n}) = \frac{1}{C} \prod_{i=1}^S \frac{\alpha_i^{n_i}}{\prod_{t=1}^{n_i} \phi_i(t)}, \quad (6)$$

being C a normalizing constant ensuring that

$$\sum_{\mathbf{1}^T \mathbf{n} = N} \pi(\mathbf{n}) = 1. \quad (7)$$

We computed C by enumerating all the possible configurations that the vector \mathbf{n} can attain.

A. Affinity estimation

The steady state distribution [Eq. (6)] can be rewritten taking into account the antigen binding affinity as

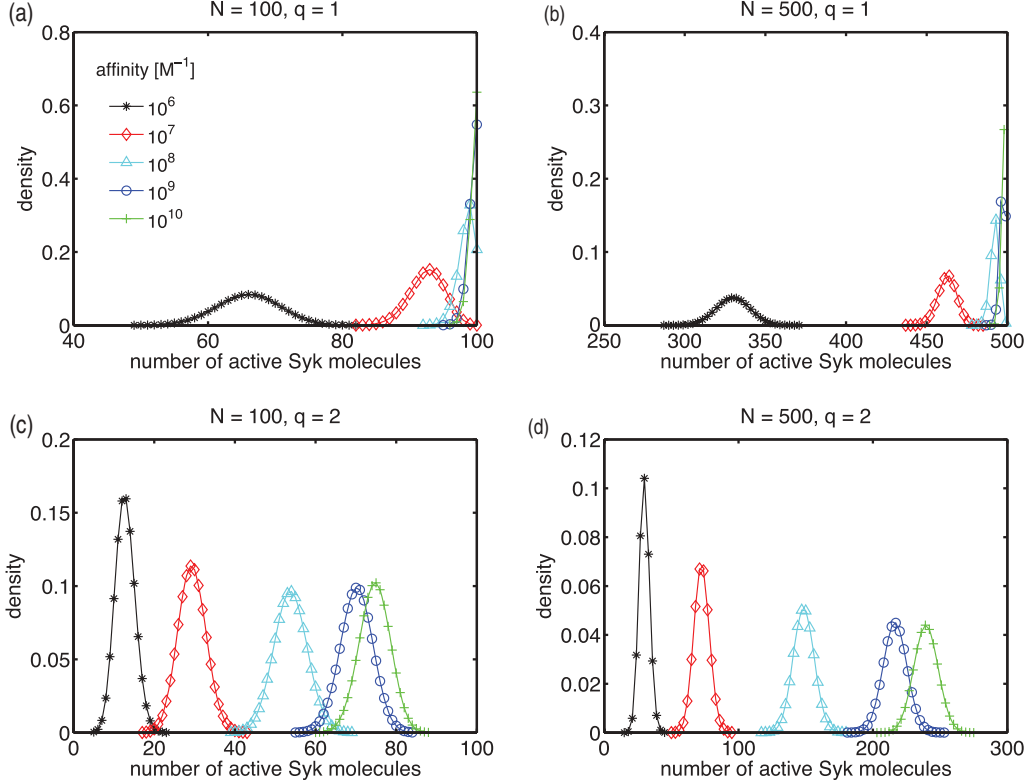


FIG. 2. (Color online) Probability density functions for the total number of active Syk molecules (n_4) for a different number of receptors, different values of the exponent q in ϕ_4 , and Ag-BCR binding affinities $\theta_1 = 10^6$ (black \star), $\theta_2 = 10^7$ (red \diamond), $\theta_3 = 10^8$ (light blue \triangle), $\theta_4 = 10^9$ (blue \circ), and $\theta_5 = 10^{10}$ (green $+$). (a),(b) For $q = 1$, the marginals in Eq. (10) are not well separated for high affinity values. (c),(d) For $q = 2$, the marginals are well separated. Furthermore, the separation between these probability distributions increases by including more receptors.

follows:

$$\pi(\mathbf{n}|\theta) = \frac{1}{C} \prod_{i=1}^S \frac{\alpha_i^{n_i}}{\prod_{t=1}^{n_i} \phi_i(t)}, \quad (8)$$

where θ is a parameter depending on k_{off} in [Eq. (4)]. With this setting, we can consider a family of probability distributions $\pi_\theta(\mathbf{n}) = \pi(\mathbf{n}|\theta)$ depending on different BCR-antigen affinity values. Let us consider the marginal distribution of the total number of activated Syk molecules (n_4) derived from the closed form steady state distribution in Eq. (6):

$$\tilde{\pi}(n_4) = \sum_{n_1+n_2+n_3=N-n_4} \pi(n_1, n_2, n_3, n_4). \quad (9)$$

Then, we are interested in the family of marginal probability distributions:

$$\tilde{\pi}_\theta(n_4) = \tilde{\pi}(n_4|\theta), \quad (10)$$

parametrized by the system input θ representing the above introduced affinity value [Fig. 2(a)–2(d)].

B. Accuracy

We consider the Jensen-Shannon divergence (JS divergence) D^{JS} [24] [a symmetrization of the Kullback-Leibler divergence (KL divergence) [25]] as a measure of the differences between the marginal distributions $\tilde{\pi}_{\theta_i}$ and $\tilde{\pi}_{\theta_j}$ (defined

in Sec. II A):

$$D^{\text{JS}}(\tilde{\pi}_{\theta_i}, \tilde{\pi}_{\theta_j}) = \frac{1}{2} \sum_{k=1}^N \tilde{\pi}_{\theta_i}(k) \log \left(\frac{\tilde{\pi}_{\theta_i}(k)}{\tilde{\pi}_{\theta_j}(k)} \right) + \frac{1}{2} \sum_{k=1}^N \tilde{\pi}_{\theta_j}(k) \log \left(\frac{\tilde{\pi}_{\theta_j}(k)}{\tilde{\pi}_{\theta_i}(k)} \right). \quad (11)$$

We analyzed the behavior of the JS divergence between the distributions π_{θ_i} , where $\theta_i = \{10^6, 10^7, 10^8, 10^9, 10^{10}\}$.

III. RESULTS AND DISCUSSION

The family of probability distributions [Eq. (10)] represents the readout of the proposed model with different input affinities. We analyze the dependence of the distribution of the number of active Syk molecules with respect to alterations of the parameter q , the number of receptors N , and the matrix H [Eq. (4)]. Some entries of H (i.e., binding affinities for Syk and Lyn) have uncertain numerical values, whereas others depend on the total concentration of antigen molecules (Sec. A). In the following, we justify the choice of the parameter value q based on experimental observations addressing the total number of active Syk molecules for different BCR binding affinities.

A. Choice of the parameter q based on experimental results

The number of active Syk molecules has been reported to strongly depend on the BCR-antigen binding affinity [6]. In

TABLE I. Values of the ratios $\frac{\mu_{\theta_{\text{high}}}}{\mu_{\theta_{\text{low}}}}$, where $\theta_{\text{high}} = 5 \times 10^8 M^{-1}$ and $\theta_{\text{low}} = 9.9 \times 10^6 M^{-1}$ for the indicated number of receptors and coefficients q of the modulating function $\phi_4(\cdot)$. Values of $q \geq 2$ are in agreement with experimental results [6].

Number of receptors	$q = 1$	$q = 1.5$	$q = 2$	$q = 2.5$
100	1.07	1.48	2.11	2.15
200	1.07	1.62	2.30	2.23
300	1.07	1.70	2.40	2.26
400	1.07	1.77	2.46	2.28
500	1.07	1.83	2.51	2.29

particular, TIRF (total internal reflection fluorescence) images have shown that recruitment of phosphorylated Syk to the contact area between the B cell and an antigen-containing bilayer is enhanced in high affinity ($5 \times 10^8 M^{-1}$) compared to low affinity ($9.9 \times 10^6 M^{-1}$) BCRs. More precisely, an ~ 2.5 -fold reduction in the total number of active Syk molecules has been observed within the contact area for low affinity BCRs compared to high affinity ones. We therefore analyzed the ratio $\frac{\mu_{\theta_{\text{high}}}}{\mu_{\theta_{\text{low}}}}$ of the total number of active Syk molecules within a single signaling unit (see Table I), where $\mu_{\theta_{\text{high}}}$ and $\mu_{\theta_{\text{low}}}$ represent the mean number of active Syk molecules for the affinity values $\theta_{\text{high}} = 5 \times 10^8 M^{-1}$ and $\theta_{\text{low}} = 9.9 \times 10^6 M^{-1}$, respectively. The value $q = 2$ captures the experimental results.

B. Sensitivity to parameter values

The binding rates of Syk ($k_{\text{on}}^{\text{Syk}}$) and Lyn molecules ($k_{\text{on}}^{\text{Lyn}}$) are fixed and reported in Table II. The unbinding rates $k_{\text{off}}^{\text{Syk}}$ and $k_{\text{off}}^{\text{Lyn}}$ are reported to be within two orders of magnitude [11,26]. The fastest unbinding rates ($10s^{-1}$) did not lead to a good discrimination accuracy. Alterations of the values of $k_{\text{off}}^{\text{Lyn}}$ did not result in a significant change in the discrimination ability [Fig. 3(a)]. Conversely, reducing the $k_{\text{off}}^{\text{Syk}}$ from $1s^{-1}$ to $0.1s^{-1}$ resulted in an increase of the JS divergence of two to three orders of magnitude for different values of q [Fig. 3(b)]. This result is remarkable due to the key role of Syk in signaling downstream to early BCR activation.

TABLE II. Values of the parameters used in the simulation. The orders of magnitude of the binding and unbinding rates are extracted from the reported references. k_{on} has been estimated according to Eqs. (A1) and (A2).

Reaction	Real value	Mapped value	Symbol	Reference
Ag-BCR (on)	$0.7\text{--}3.8 \times 10^6 M^{-1} s^{-1}$	$25\text{--}1000s^{-1}$	k_{on}	[11,28]
Ag-BCR (off)	$0.7\text{--}3.8 \times 10^{-4} s^{-1}$	$0.7\text{--}3.8 \times 10^{-4} s^{-1}$	k_{off}	[5]
Lyn (on)	$\sim 10^7 M^{-1} s^{-1}$	$1.4s^{-1}$	$k_{\text{on}}^{\text{Lyn}}$	[31]
Lyn (off)	$10\text{--}0.1s^{-1}$	$1s^{-1}\text{--}0.1s^{-1}$	$k_{\text{off}}^{\text{Lyn}}$	[26]
Syk (on)	$\sim 10^7 M^{-1} s^{-1}$	$24s^{-1}$	$k_{\text{on}}^{\text{Syk}}$	[26,31]
Syk (off)	$10\text{--}0.1s^{-1}$	$1s^{-1}\text{--}0.1s^{-1}$	$k_{\text{off}}^{\text{Syk}}$	[11]
	4×10^5		N_{BCR}	[26]
	1.6×10^6		N_{Syk}	[26]
	2.8×10^4		N_{Lyn}	[26]

C. Simplified signaling pathway

We consider a simplified version of the pathway described in Fig. 1 consisting of two states only, namely, the unbound (s_1) and the antigen-bound (s_2) BCR [Fig. 1(a)]. We are interested in testing whether this simplified pathway exhibits the same ability to discriminate the affinity spectrum as the full length one. Due to the lack of experimental data on the dependence of antigen unbinding events on the number of antigen-bound BCRs, a natural choice for the modulating functions $\phi_1(\cdot)$ and $\phi_2(\cdot)$ would be the identity, e.g., $q = 1$. Nonetheless, we analyzed the affinity discrimination ability for different values of q . Interestingly, by setting $q = 2$ the simplified pathway shows a discrimination ability comparable to the full pathway [Fig. 4(a)]. However, the robustness of this system with respect to alterations of antigen concentrations is strongly reduced. Indeed, increasing the value of k_{on} from $100 s^{-1}$ to $1000 s^{-1}$ results in an increase of the JS divergence by two orders of magnitude for the simplified signaling pathway, whereas no significant difference is obtained for the full length pathway [Fig. 4(a)]. Notably, the value $q = 1$ is unable to produce values of JS divergence that translate into a robust cellular response for high affinities in both simplified and full length pathways. Nevertheless, the full length pathway is still robust to alterations of k_{on} when compared to the simplified pathway [Fig. 4(b)].

D. Dependence on the number of receptors within a signaling unit

Experimental results have shown that upon antigen binding BCRs arrange in microclusters on the B-cell surface [9,15]. Here we study the effect of the number N of BCRs within a single signaling unit on the affinity discrimination. To this purpose, we analyzed the increment of the JS divergence as a function of N and computed its discrete derivative with respect to N :

$$\left. \frac{\Delta JS}{\Delta N} \right|_{N_i} = \frac{JS(N_{i+1}) - JS(N_i)}{N_{i+1} - N_i}. \quad (12)$$

By analyzing the behavior of the JS divergence [Fig. 5(a)] we observe that allocating an increasing number of receptors within a single signaling unit results in an increase of the cellular capability to discriminate between high range

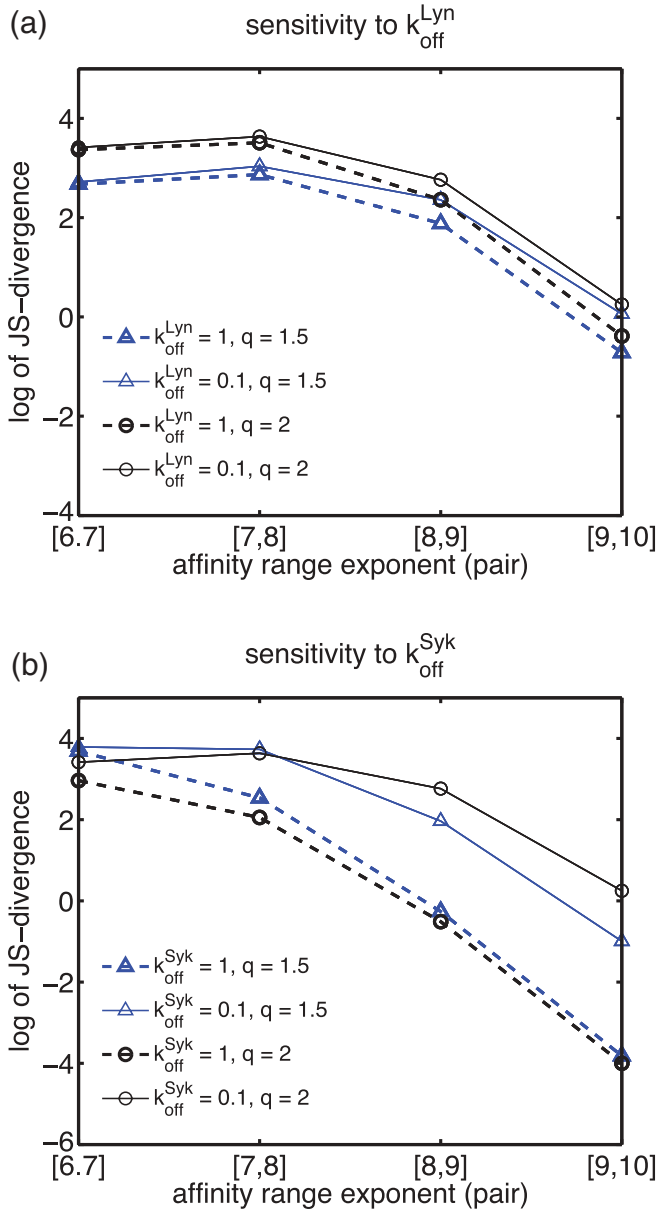


FIG. 3. (Color online) Sensitivity to parameter values. Logarithm of the JS divergence for the pair of affinities listed on the x axis ($[p, p + 1]$ maps to $[10^p - 10^{p+1}]$) upon altering $k_{\text{off}}^{\text{Lyn}}$ (a) and $k_{\text{off}}^{\text{Syk}}$ (b). Different lines correspond to different parameter sets as [(a),(b)] $k_{\text{off}}^{\text{Syk/Lyn}} = 1s^{-1}$, $q = 1.5$ (dashed blue Δ), $k_{\text{off}}^{\text{Syk/Lyn}} = 0.1s^{-1}$, $q = 1.5$ (solid blue Δ), $k_{\text{off}}^{\text{Syk/Lyn}} = 1s^{-1}$, $q = 2$ (dashed black \circ), $k_{\text{off}}^{\text{Syk/Lyn}} = 0.1s^{-1}$, $q = 2$ (solid black \circ). The system is robust with respect to alterations of $k_{\text{off}}^{\text{Lyn}}$ and k_{on} , whereas alterations of $k_{\text{off}}^{\text{Syk}}$ are crucial in the affinity discrimination.

affinities ($10^9 M^{-1} - 10^{10} M^{-1}$). However, such an increase is sublinear for values of $q \geq 2$. Remarkably, the best affinity discrimination for N between 100 and 500 is achieved with $q = 2$, in agreement with experimental results [15]. For this parameter value there exists a critical value of N above which the discrete derivative of the JS divergence decreases [Fig. 5(b)].

The JS divergence of two n -dimensional distributions $\mathbf{p} = (p_1, \dots, p_n)$ and $\mathbf{q} = (q_1, \dots, q_n)$, whose marginals are

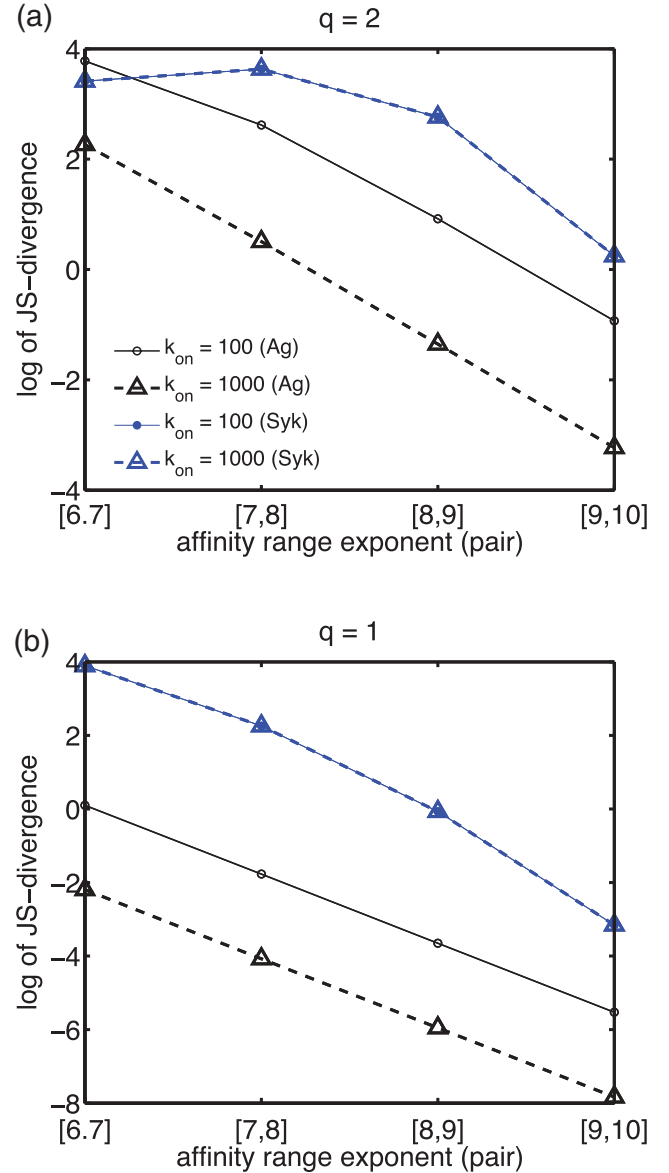


FIG. 4. (Color online) Logarithm of the JS divergence for the pair of affinities listed on the x axis ($[p, p + 1]$ maps to $[10^p - 10^{p+1}]$) for $q = 2$ (a) and $q = 1$ (b). $k_{\text{on}} = 100s^{-1}$ for the pathway consisting of s_1 and s_2 only (Ag) (solid black \circ); $k_{\text{on}} = 1000s^{-1}$ for the (Ag) pathway (dashed black Δ); $k_{\text{on}} = 100s^{-1}$ for the pathway up to s_4 (Syk) (solid blue \bullet); $k_{\text{on}} = 1000s^{-1}$ for the (Syk) pathway (dashed blue Δ). The pathway up to Syk is more robust than the one consisting of antigen binding only with respect to alterations of k_{on} .

independent and identically distributed is [25]

$$D^{\text{JS}}(\mathbf{p}, \mathbf{q}) = nD^{\text{JS}}(p_i, q_i). \quad (13)$$

By assuming independence between the signaling units, it follows from Eq. (13) that the JS divergence increases linearly with the number of clusters. The number of clusters is reported to be around 20–25, each consisting of 100–500 BCRs [15]. Our model suggests that the optimal number of BCRs to be allocated in a single unit is within the range [100, 150]. Values of N within this range maximize the discrete derivative of the JS divergence. Additionally, this result potentially explains the reason for the organization of BCRs in multiple signaling

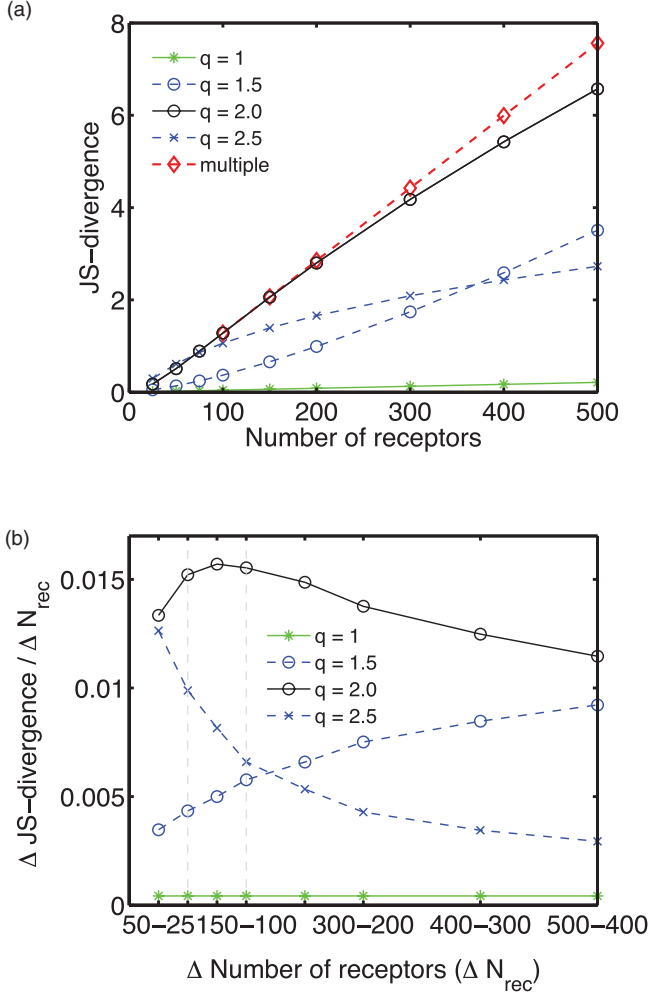


FIG. 5. (Color online) Behavior of the JS divergence (a) and the discrete derivative of the JS divergence (b) between distributions resulting from high affinity values ($10^9 M^{-1}$ and $10^{10} M^{-1}$) as a function of the total number of receptors within a signaling unit. Different lines correspond to different values of q in ϕ_4 : $q = 1$ (solid green \star); $q = 2$ (dashed blue \circ); $q = 2$ (solid black \circ); and $q = 2.5$ (dashed blue \times). (a) The dashed red \diamond line shows the theoretical linear increase of the JS divergence that would be obtained by extending the segment yielding the maximum discrete derivative in (b). (b) The range of the optimal number of BCRs to be allocated in a signaling unit falls between the vertical dashed lines.

units. Indeed, given N receptors, their arrangement in clusters of size within the range [100,150] leads to a better affinity discrimination than a single signaling unit having the same number of BCRs [Fig. 5(a)].

IV. CONCLUSIONS

In this work, we investigated a possible mechanism explaining the specificity of BCRs at high antigen binding affinities. We did not explicitly model the spatial component in the distribution of receptors within a single signaling unit, since our focus was not on the causes driving the formation of BCR microclusters, discussed in Refs. [6,9,15]. Instead, we were interested in how a system consisting of several receptors

and early signaling molecules is able to give rise to different equilibrium distributions depending only on ligand binding affinity. Thus, we performed our analyses by considering a fixed number of BCRs within each signaling unit, early signaling states, and relevant transitions. Receptors are modeled as queuing customers and their possible states are colonies. Such colonies constitute a network of queues. The assumptions we made on the network topology and on the transitions between colonies enabled us to exploit a convenient factorization of the steady state distributions of each queue [16]. Our model captures the downstream signaling role of Syk molecules [6,18] in a signaling unit through a nonlinear modulating function. This allows one to generate different levels of Syk activation in response to antigen affinity values spanning four orders of magnitude. Additionally, our results suggest that an optimal number of BCRs in a single signaling unit is rather towards lower bounds of experimental observations [15]. A possible limitation of the presented framework is the necessity of relying on equilibrium distributions for clusters of fixed size, without accounting for the biological processes leading to the affinity-dependent formation of clusters [19,27]. Computational limitations currently hamper the extension of the signaling pathway as well as the addition of more receptors inside a single signaling unit because of the combinatorial complexity of the state space defined in Eq. (2). Overcoming these difficulties will constitute a valuable step towards the analysis of longer pathways, making the proposed model (Sec. II) suitable for applications to other contexts involving cellular signaling.

ACKNOWLEDGMENTS

This research was supported by a SystemsX grant to the InfectX RTD. F.F. thanks Dagmar Iber for helpful discussion in understanding the peculiarity of B cells. F.C. thanks Renato Paro for having kindly supported this work.

APPENDIX

The parameters used in the simulations are reported in Table II and have been extracted from [11,28], and references therein. The main issue is to identify suitable values for the ratio $k_{\text{on}}/k_{\text{off}}$. In the following, we map the value of the dissociation constant K_D to suitable values of k_{on} and k_{off} . The latter follows directly from the experimental observations that the half-life of antigen (Ag)-BCR complexes is ~ 1 s for an affinity value of $10^6 M^{-1}$ and in the order of 30 min for an affinity value of $10^{10} M^{-1}$ [5] (Table II). Since differences in binding affinity depend only on k_{off} [21,22], we determine a suitable value of k_{on} . The value of k_{on} is the result of both the *encounter rate* of a BCR and an Ag molecule and their *reaction rate* [28]. Assuming that the reaction rate is the limiting step, the values of k_{on} can be determined by finding the collision time between a BCR and an Ag molecule. For this purpose, we exploit the simulation setting described in Refs. [11,29], where a square of size $1.5 \mu\text{m}$, a given number N_{Ag} of Ag molecules, and BCRs were considered. Each Ag molecule is supposed to occupy the

center of a circle, having radius

$$r = \sqrt{\frac{A}{N_{\text{Ag}}\pi}} \quad (\text{A1})$$

so that the area A is fully covered by the union of those circles. Next, we consider one annulus having outer radius given by Eq. (A1) and inner radius s , e.g., the radius of an Ag molecule, in the order of ~ 5 nm. The outer circle of the annulus has a reflecting boundary, whereas the inner boundary is absorbing. A BCR undergoes Brownian diffusion in the annulus. Berg and

Purcell [30] computed the average time required for a BCR to meet an Ag molecule as

$$\tau = \frac{r^4}{2D_r(r^2 - s^2)} \log \frac{r}{s} - \frac{3r^2 - s^2}{8D_r}, \quad (\text{A2})$$

where $D_r = D_{\text{Ag}} + D_{\text{BCR}} = 2 \times 0.1 \mu\text{m}^2/\text{s}$ is the resulting diffusion coefficient of a BCR and an Ag molecule [11]. Different numbers of Ag molecules map to different mean capture times. In particular, 100 Ag molecules on A correspond to a mean capture time of $\sim 1/25s$, 500 to $\sim 1/200s$, 1000 to $\sim 1/600s$, and 2000 to $\sim 1/1000s$.

-
- [1] B. Alberts, A. Johnson, J. Lewis, M. Raff, K. Roberts, and P. Walter, *Molecular Biology of the Cell*, 5th ed. (Garland Science Taylor & Francis Group, New York, 2007).
- [2] F. Burnet, *Ca-Cancer J. Clin.* **26**, 119 (1976).
- [3] Melvin Cohn, N. Av Mitchison, William E. Paul, Arthur M. Silverstein, David W. Talmadge, and Martin Weigert, *Nat. Rev. Immun.* **7**, 823 (2007).
- [4] H. Niiri and E. A. Clark, *Nat. Rev. Immun.* **2**, 945 (2002).
- [5] F. D. Batista and M. S. Neuberger, *Immunity* **8**, 751 (1998).
- [6] W. Liu, T. Meckel, P. Tolar, H. W. Sohn, and S. K. Pierce, *J. Exp. Med.* **207**, 1095 (2010).
- [7] M. R. Sebastian Herzog and H. Jumaa, *Nat. Rev. Immun.* **9**, 195 (2009).
- [8] G. Aquino, D. Clausnitzer, S. Tollis, and R. G. Endres, *Phys. Rev. E* **83**, 021914 (2011).
- [9] S. Fleire, J. Goldman, Y. Carrasco, M. Weber, and D. Bray, *Science* **312**, 768 (2006).
- [10] J. Yang and M. Reth, *Nature (London)* **467**, 465 (2010).
- [11] P. K. Tsourkas, W. Liu, S. C. Das, S. K. Pierce, and S. Raychaudhuri, *Cell. Mol. Immunol.* **9**, 62 (2011).
- [12] T. McKeithan, *Proc. Natl. Acad. Sci. USA* **92**, 5042 (1995).
- [13] J. Wedagedera and N. J. Burroughs, *Biophys. J.* **91**, 1604 (2006).
- [14] J. F. Keane and L. E. Atlas, *International Conference on Acoustics, Speech, and Signal Processing* (IEEE, Orlando, FL, 2002), Vol. 2, pp. II-1597–II-1600.
- [15] D. Depoil, S. Fleire, B. L. Treanor, M. Weber, N. E. Harwood, K. L. Marchbank, V. L. J. Tybulewicz, and F. D. Batista, *Nat. Immun.* **9**, 63 (2008).
- [16] F. P. Kelly, *Reversibility and Stochastic Networks* (Cambridge University Press, Cambridge, England, 2011).
- [17] R. G. Endres and N. S. Wingreen, *Phys. Rev. Lett.* **103**, 158101 (2009).
- [18] D. Fooksman and M. Dustin, *J. Exp. Med.* **207**, 907 (2010).
- [19] F. D. B. Naomi E. Harwood, *Immunity* **28**, 609 (2008).
- [20] A. K. Erlang, *Nyt Tidsskrift Matematik* **20**, 33 (1909).
- [21] J. P. Ways and P. Parham, *Biochem. J.* **216**, 423 (1983).
- [22] G. I. Bell, *Nature (London)* **248**, 430 (1974).
- [23] G. R. Grimmett and D. R. Stirzaker, *Probability and Random Processes* (Oxford University Press, New York, 2001).
- [24] J. Lin and S. K. M. Wong, *Int. J. Gen. Syst.* **17**, 73 (1990).
- [25] S. Kullback and R. A. Leibler, *Ann. Math. Stat.* **22**, 79 (1951).
- [26] B. Goldstein, J. R. Faeder, W. S. Hlavacek, M. L. Blinov, A. Redondo, and C. Wofsy, *Mol. Immunol.* **38**, 1213 (2002).
- [27] A. S. Reddy, P. K. Tsourkas, and S. Raychaudhuri, *Cell. Mol. Immunol.* **8**, 255 (2011).
- [28] G. Nudelman, M. Weigert, and Y. Louzoun, *Mol. Immunol.* **46**, 3141 (2009).
- [29] P. K. Tsourkas, N. Baumgarth, S. I. Simon, and S. Raychaudhuri, *Biophys. J.* **92**, 4196 (2007).
- [30] H. Berg and E. Purcell, *Biophys. J.* **20**, 193 (1977).
- [31] J. R. Faeder, W. S. Hlavacek, I. Reischl, M. L. Blinov, H. Metzger, A. Redondo, C. Wofsy, and B. Goldstein, *J. Immunol.* **170**, 3769 (2003).